ELSEVIER

Journal of Non-Crystalline Solids 171 (1994) 46–52

JOURNAL OF NON-CRYSTALLINE SOLIDS

Sol to gel reaction in the K_2O–Al_2O_3–SiO_2 system

K.J. Lee [a], T.Y. Tien [a], E. Gulari [b]

[a] *Department of Material Science and Engineering and* [b] *Department of Chemical Engineering, University of Michigan, Ann Arbor, MI 48109-2136, USA*

Received 8 November 1993; revised manuscript received 10 February 1994

Abstract

A sol to gel transition reaction of three metal alkoxides with water in the preparation of gel in the K_2O–Al_2O_3–SiO_2 system was investigated using in situ viscosity measurements and the Raman scattering technique. The viscosity measurements reveal that the viscosity of the solution and the dependence of the reduced viscosity on polymer concentrations change abruptly near the gelation point. The Raman scattering results suggested that the hydrolysis of the TMOS was the rate-limiting step of the overall reaction. It was also found that a basic solution with excess amounts of water was needed to synthesize a transparent crack-free gel.

1. Introduction

The sol–gel process is now a well-recognized technique for making glass at a relatively low temperature without melting [1–4]. This technique is applicable to single-component oxide glasses [5–7] as well as multicomponent oxide glasses [8–11] using metal alkoxides as precursors. The metal alkoxides form gels through hydrolysis accompanied by polycondensation reactions and then gels are converted to the oxide glasses by heat treatments.

In spite of the higher costs of metal alkoxides and difficulties such as slow drying rate, residual organic and material handling difficulties, the sol–gel process has been used to form glasses because of its many distinctive advantages [3]. These include high purity, better homogeneity and, especially, the feasibility of preparing multicomponent glasses and ceramics at lower temperatures than in conventional methods [12]. Since each metal alkoxide has a different reaction rate, the overall reaction must be controlled to maintain the homogeneity of the gels formed by hydrolysis and polycondensation of metal alkoxides [13]. The reaction is sensitive to variables such as concentrations of alkoxides, water, solvents, reaction temperature, pH of the solution and mixing sequences of each component [7,14–16]. Optimum reaction conditions can only be established by trial and error manipulation of these variables.

The dependence on these variables in sol to gel transition is more crucial than in gel to glass conversion. The conversion of dried gels to oxide glasses has been studied extensively but there are few reports in the literature dealing with the sol to gel transition of metal alkoxides [17–19]. The main objective of this study was to investigate the

* Corresponding author. Tel: +1-313 764 9449. Telefax: +1-313 763 4788.

0022-3093/94/$07.00
SSDI 0022-3093(94)00141-9

sol to gel transition reaction in a ternary metal alkoxides system through hydrolysis and polycondensation reactions. The most distinctive phenomenal change during the sol to gel transition is the viscosity change. This change was measured in our studies by the falling ball method. The viscosity changes was correlated with the kinetic information of transition reaction obtained by Raman scattering intensities. Conditions for synthesizing transparent monolithic gels were also investigated.

2. Experimental procedure

2.1. Alkoxides solution preparation

The starting materials used to prepare the alkoxide solutions were potassium methoxide $KOCH_3$ [1], aluminum sec-butoxide $Al(OC_4H_9)_3$ [1], and tetramethoxysilane {TMOS, $Si(OCH_3)_4$} [2]. Their molar ratios were adjusted to have a potash feldspar composition of $K_2O \cdot Al_2O_3 \cdot 6SiO_2$. $Si(OCH_3)_4$ was initially dissolved in methanol [1] as a solvent and formamide [1] was added as a drying control additive to prevent cracks during drying [20]. The TMOS solution was vigorously stirred and $K(OCH_3)$ was added to the solution. Stirring was continued while the $Al(OC_4H_9)_3$ solution was added. The mixing of the alkoxides solutions was processed under a nitrogen atmosphere at 80°C. After the clear solution was formed, it was cooled to room temperature and then hydrolyzed by adding distilled water drop by drop. In some of the batches, HNO_3 was used as an acid catalyst. Several concentrations of the mixtures of solvent, drying control additives, water and catalyst were evaluated for their formation of transparent and crack-free monolithic dried gels.

2.2. Viscosity measurement

The alkoxide solutions were transferred into a long-necked flask which was located between two photo sensors [3]. The sensors were U-shaped photocell-operated and were the dark-on type. One tip of the U-shaped sensor was the light source and the other was the detector. The neck of the flask was placed between the sensors in such a way that, when the metal ball was dropped, it blocked the source light. Two sensors were clamped to a support so that the vertical distance between them was adjustable. Both sensors were connected to a timer–counter [4]. When the metal ball was dropped from the top surface of the solution in the flask, it triggered the two sensors sequentially. The time interval between the two triggering events was recorded on the timer–counter throughout the transition reaction of the sol to gel until the metal ball could no longer move downward from the top of the gelled surface.

The time interval, i.e., the traveling time of the ball between two points in the fluid, was used as an empirical unit of the viscosity of the fluid because the traveling time can be related to the viscosity by Stoke's law:

$$\eta = F/6\pi rv = (m-m_0)g/6\pi rv, \qquad (1)$$

where η is the liquid viscosity and m and r are the mass and radius of the metal ball, respectively, m_0 is the mass of liquid displaced by the metal ball and v is the falling rate (terminal velocity) of the ball. By assuming that the densities of the metal ball and the liquid are constant with time, Eq. (1) can be rewritten as

$$\eta = C_1/v\mu C_1/(\mathrm{D}t/\mathrm{D}x) \qquad (2)$$

and

$$C_1 = (2/9)r^2g(r_S - r_l)$$

where r_s and r_l are the densities of the ball and the liquid, respectively, t is the traveling time and x is the traveling distance. According to Eq. (2), the viscosity of the liquid is proportional to the falling time of the ball per unit distance. Thus, the time interval measured by the timer–counter

[1] Aldrich Chemical Co., Milwaukee, WI, USA.
[2] Alfa Products, Danvers, MA, USA.
[3] Model FE8V, Microswitch, Freeport, IL, USA.
[4] Model 5328B, Hewlett–Packard, Corvallis, OR, USA.

Table 1
Gelation time t_γ, for different sols

Sols	pH	t_g	Appearance
alkoxides + H_2O + HNO_3	3.5	2 h	opaque
alkoxides + H_2O + CH_3OH	8.0	20 h	translucent
alkoxides + H_2O + CH_3OH + HNO_3	3.0	0.5 h	opaque
alkoxides + H_2O + CH_3OH + $CHONH_2$	9.6	2 h	transparent
alkoxides + H_2O + CH_3OH + $CHONH_2$ + HNO_3	4.5	1 h	translucent

can be interpreted as the empirical viscosity of the solution. In order to minimize errors, different sized metal balls were dropped in different cross-sectional area containers. The data were reproduced at least ten times and they were accurate to within 5%. They were then averaged for each datapoint presented in this paper.

For measurements at higher temperatures, the viscosity measurement was performed inside the flask while the temperature was maintained at 55 ± 2°C by circulating heated water around the outside of the double-jacketed flask. The lower-temperature viscosity was measured in a regular flask which was immersed an ice bath and then kept in a refrigerator to hold the temperature at 0°C. The flask was taken out periodically to drop the metal balls and refrigerated again. This procedure required less than 2 min.

The reduced viscosity of a polymeric solutions, η_{sp}/C, has a relationship with the concentration of the polymer in solution (g/dl) according to Huggins' equation [21]:

$$\eta_{sp}/C = [\eta] + k[\eta]^2 C, \tag{3}$$

with

$$\eta_{sp} = \eta_{rel} - 1 = \eta/\eta_0 - 1,$$

where η_{sp} is the specific viscosity, C is the polymer concentration (g/dl), $[\eta]$ is the intrinsic viscosity and k is the proportional constant. η_{rel} is the relative viscosity, which is the ratio of the viscosity of the solution, η, to the viscosity of the solvent, η_0. Eq. (3) was applied to obtain information regarding the formation of the polymer structure. If polymers dissolved in the solution are linear, the reduced viscosity is proportional to the concentration of the polymers, as in Eq. (3). However, if the polymers are spherical or a 3D network structure, the reduced viscosity is independent of polymer concentration [17].

2.3. Raman scattering

The Raman scattering measurements were made in situ using Raman spectroscopy [5] with a 488 nm Ar ion laser. Operating conditions were 250 mW of output power with a 1.2 cm^{-1} slit and a 4 cm^{-1} scanning interval. Sample solutions were transferred to the glass tube, then sealed and located in the spectroscope throughout the experiment. The spectra were collected every 15 min until gelation and transferred at that time to the computer for analysis. The normalized intensity of the Raman band using internal standard is accurate to within 10%.

Since the Raman scattering intensity of a characteristic band is proportional to the concentration of the scattering species, the ratio of intensity at time 0 and time, t, can be written as

$$I(t)/I(0) = C(t)/C(0), \tag{4}$$

where I and C are the intensity and concentration, respectively.

3. Results

Table 1 gives the results where pH, gelation time and the appearance of solutions with different batches are listed. The amount of water used was ten times the stoichiometric amount needed for hydrolysis. The volume ratio of methanol to formamide to total alkoxides was 1.5 : 1 : 1, and

[5] Spex Industrial Inc., Metuchen, NJ, USA.

the molar ratio of HNO_3 to alkoxides was 0.2 when HNO_3 was used. The solution with methanol and formamide was found to be the most successful for preparing transparent monolithic gels. The basicity of the solution was due to formamide and the potassium ions.

In order to investigate the effects of the acid catalyst, different acid concentrations were used with the methanol–formamide solution. The gelation time observed was 2 h for the solution without HNO_3, 1 h for a 0.2 mol ratio of HNO_3 to alkoxides and 10 min for a 0.4 mol ratio of HNO_3 to alkoxides. Apparently, the higher the acid concentration, i.e., the lower the pH value, the shorter the time needed to form a gel.

The methanol–formamide solution was chosen for in situ viscosity studies. Viscosity changes at different temperatures, 0, 25, and 55°C were plotted against time, as shown in Fig. 1. In this figure, the vertical axis represents the empirical viscosity, which was the time taken for the ball to travel the unit distance in the solution. The end point of the viscosity was the gelling point when the ball was unable to move downward. Metal balls of 5, 8, and 9.5 mm diameter were used for the viscosity measurement. Measurements results using flasks with different cross-section area were essentially

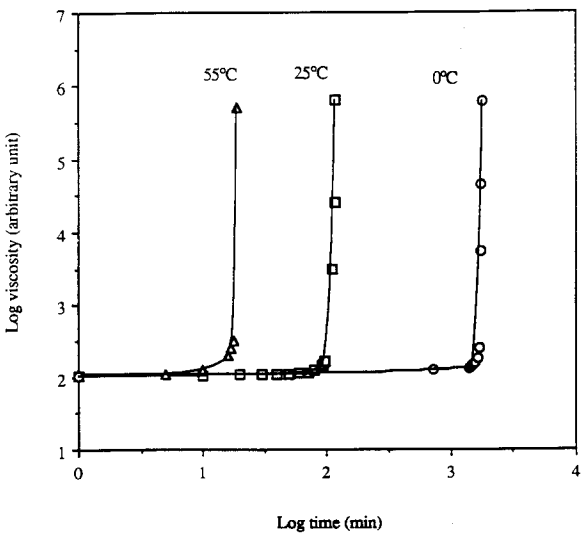

Fig. 1. Viscosity changes with time at different temperatures show abrupt increases near the gelation point. Lines are drawn as a guide to the eye.

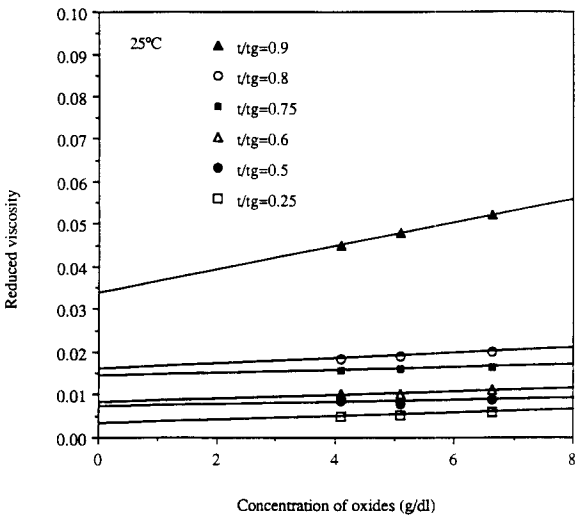

Fig. 2. Dependence of reduced viscosity on concentration of oxides demonstrates a linear relationship near the gelation point. The data is fitted to the linear function of oxides concentration. The correlation factor, $R = 0.99$ or better for all fittings.

the same except for the scale factor of the vertical axis. Fig. 1 also shows that the viscosity of the solution increased very slowly until the onset of gelation. After the gelation point was reached, the viscosity was independent of temperature. It took longer for gelation to occur at lower temperatures. This was expected because the reaction rate follows the Arrhenius equation, $k \propto \exp(1/T)$.

In Fig. 2, the reduced viscosity, η_{sp}/C obtained from the empirical viscosity measured by the falling ball method, is plotted against the concentration of oxides during the sol to gel transition. These results were fitted to Eq. (3). The effect of the oxide concentration on the reduced viscosity is negligible until the later stage of transition where t/t_g is 0.9.

Typical Raman spectrum of the sol in the low wave number region is presented in Fig. 3 along with assignments for each characteristic band. In order to obtain information on kinetics of hydrolysis, the band at 640 cm^{-1}, which was the Si–O–C stretching mode of TMOS, was used for quantitative studies since it diminished as the sol changed to gel. Other TMOS bands and potassium

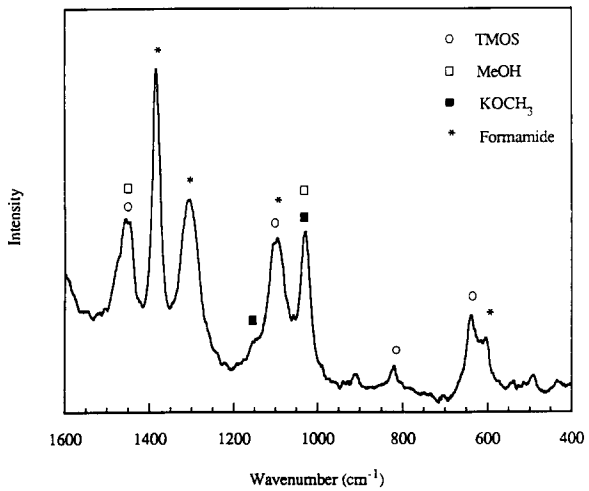

Fig. 3. Raman spectrum of solution at the beginning of the reaction along with the assignments of characteristic bands.

methoxide bands overlapped to some extent, with bands from the alcohol which was present in large amounts as the solvent. K–O–C and Al–O–C bands were undetectable in this wave number region due to the low concentration of alkoxides compared with water, alcohol and formamide.

Fig. 4 shows the changes of peak intensity of an extended peak near 640 cm^{-1} during the sol to gel reaction. Since this peak overlapped with the formamide band at 613 cm^{-1}, they were deconvoluted in order to obtain the integrated intensity of the TMOS band at 640 cm^{-1}. The integrated intensity of the TMOS band at 640 cm^{-1} with reduced time is plotted in Fig. 5. It revealed that the TMOS band existed until nearly the end of gelation. No partially hydrolyzed TMOS bands were found in the Raman spectrum. To obtain the rate constant of the

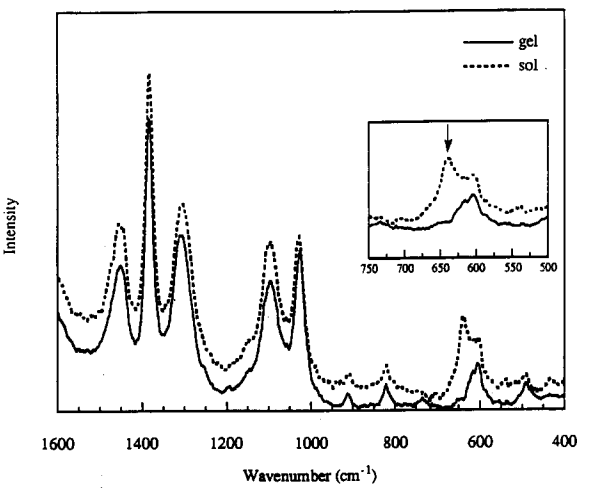

Fig. 4. Raman spectra of sol and gel with the extended peak of TMOS at 640 cm^{-1}, as indicated by the arrow.

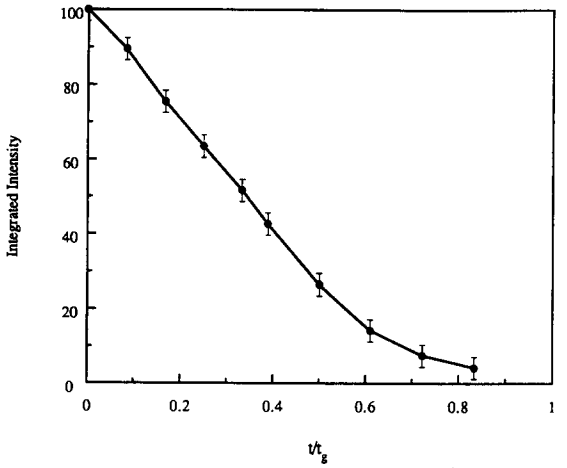

Fig. 5. Integrated Raman intensity of TMOS at 640 cm^{-1} versus reduced time. It shows the existence of TMOS until the gelation point is nearly reached. The line is drawn as a guide to the eye.

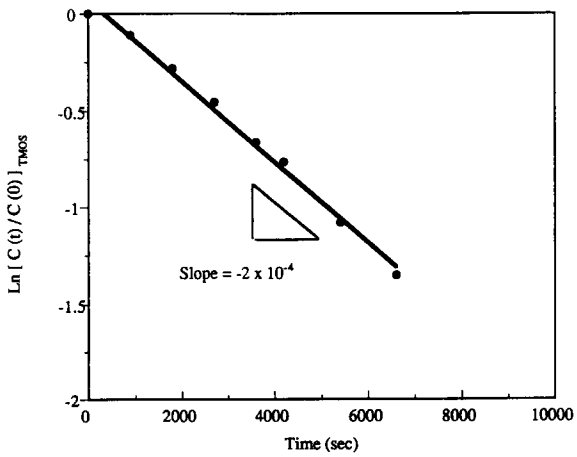

Fig. 6. Linearized intensity of TMOS at 640 cm^{-1} versus time. Based on the assumption of the first-order kinetics of the hydrolysis of TMOS. The data are fitted by the least-squares regression method. The standard error is 0.003 and the correlation factor, $R = 0.996$.

hydrolysis of TMOS, the TMOS band at 640 cm^{-1} was normalized using the formamide band at 1300 cm^{-1} as an internal standard [22]. The normalized intensity was then linearized by assuming that the hydrolysis of TMOS is pseudo first-order reaction kinetics due to excess water, i.e.,

$$\ln[C(t)/C(0)]_{TMOS} = -kt. \quad (5)$$

As shown in Fig. 6, the data are in good agreement with Eq. (5) when the linearized intensity is plotted against the real time. Thus the hydrolysis of TMOS is the first-order kinetics and the reaction rate constant, $k = 2 \times 10^{-4}$ s^{-1}.

4. Discussion

Table 1 shows the conditions to form transparent monolithic crack-free dried gels. These results indicated that slightly basic solution with excess water without the catalyst were needed to form transparent monolithic crack-free dried gels. The formamide is an organic base and thus favors condensation reaction like the base catalyst. It involves the attack of a nucleophilic deprotonated species on a neutral species. Most likely formamide is the species that deprotonated metal alkoxides due to its physical properties such as higher dipole moment hence higher dielectric constant than those of water and methanol. As a result, the gelation time of the solution containing formamide and methanol was shorter (2 h) than that of the solution containing methanol only without formamide (20 h). However, reaction mixtures with formamide under acidic conditions behave differently because it forms a stronger hydrogen bonding with the acidic catalyst and thus reduces the effective catalytic activity. Therefore, the combination of formamide with HNO_3 showed a longer gelation time (1 h) compared with the solution with HNO_3 only without formamide (0.5 h) but a shorter gelation time than that of the solution with methanol only (2 h). It has been reported by several researchers that the excess water is required to prepare bulk glasses, because an increase in the amount of water increases the degree of polymerization, leading to higher oxide content and network connectivity [23–26].

It was also observed that the higher the acid concentration, the shorter the time needed to form a gel. In the acid catalyzed reaction, the hydronium ion, H_3O^+, accelerates the reaction by an electrophilic reaction. Since the reaction rate was governed by the concentration of the hydronium ion in the solution, the higher the HNO_3 concentration, the faster the reaction rate.

The viscosity change with time and reduced viscosity dependency on the oxides concentration as shown in Figs. 1 and 2 indicate that the isolated primary particle formation occurs at the beginning of the reaction to near the gelation point and then a structure was built by aggregation of these primary particles. The linear dependence of the reduced viscosity on the oxides concentration in the later stage of the reaction ($t/t_g = 0.9$) was due to the aggregation of the primary particles instead of formation of linear polymers since the system contains excess water. It is not likely to form the linear polymers if the system contains excess water, since there is a larger amount of water than the stoichiometry needed to hydrolyze the alkoxides. The complete hydrolysis and the polycondensation in all directions are more likely rather than linear polymer formation.

Fig. 5 shows that the TMOS band persisted until near the end of gelation. This indicates that the hydrolysis continues to the end of the sol to gel reaction. No partially hydrolyzed TMOS bands were found in the Raman spectrum during the reaction, although they were not expected to be strong lines due to the similarity with the spectrum of the solvent. This result suggests that the hydrolyzed TMOS is immediately consumed by the condensation reaction as soon as it is formed. Consequently, there is always enough hydrolyzed TMOS available for condensation. This leads to the conclusion that the hydrolysis is the rate-limiting step. Since the hydrolysis of TMOS is believed to be the slowest among those of the alkoxides, the hydrolysis of TMOS is the rate-limiting step of the overall reaction.

Based on the results from the viscosity measurements and the Raman scattering technique,

one can conclude that discrete small primary particles formed first during the reaction and then aggregated between them forming a ramified structure.

5. Conclusion

The sol to gel transition of the composition K_2O–Al_2O_3–$6SiO_2$ was studied by in situ viscosity measurements and the Raman scattering technique. The abrupt changes of viscosity and the negligible dependence of reduced viscosity on oxide concentrations until the gelation point is nearly reached at $t/t_g = 0.9$ indicate that isolated primary particles were formed first and then followed by aggregation, producing the large ramified network structure. The negligible viscosity change throughout the reaction and the persistence of the TMOS Raman band until the gelation point are the results of the hydrolysis of TMOS being the rate-limiting step of the overall reaction.

This research was partially supported by National Institute of Health, National Institute of Dental Research, Specialize Materials Science Research Center No. DE-09296.

References

[1] R. Roy, J. Am. Ceram. Soc. 52 (1969) 344.
[2] S. Sakka, in: Science of Ceramic Chemical Processing, ed. L.L. Hench and D.R. Ulrich (Wiley, New York, 1986) p. 163.
[3] Ram C. Mehrotra, Mater. Res. Soc. Symp. Proc. 121 (1988) 81.
[4] B.E. Yoldas, J. Mater. Sci. 14 (1979) 1843.
[5] S. Sakka and K. Kamiya, J. Non-Cryst. Solids 42 (1980) 403.
[6] M. Yamane, S. Aso and T. Sakaino, J. Mater. Sci. 14 (1979) 607.
[7] M. Nogami and Y. Moriya, J. Non-Cryst. Solids 37 (1980) 191.
[8] J. Covino, F.G.A. DeLaat and R.A. Welsbie, Mater. Res. Soc. Symp. Proc. 73 (1986) 135.
[9] B.E. Yoldas, J. Non-Cryst. Solids 38&39 (1980) 81.
[10] F. Pancrazi, J. Phalippou, F. Sorrentino and J. Zarzycki, J. Non-Cryst. Solids 63 (1984) 81.
[11] Z. Jiang, L. Hou, F. Gan and C. Zhu, J. Non-Cryst. Solids 63 (1984) 105.
[12] K. Nakazawa, S. Inoue and M. Yamane, J. Non-Cryst. Solids 48 (1982) 153.
[13] Shyama P. Mukerjee, J. Non-Cryst. Solids 63 (1984) 35.
[14] M. Prassas and L.L. Hench, in: Ultrastructure Processing of Ceramics, Glasses, and Composites, ed. L.L. Hench and D.R. Ulrich (Wiley, New York, 1984) p. 100.
[15] J.D. Mackenzie, in: Ultrastructure Processing of Ceramics, Glasses, and Composites, ed. L.L. Hench and D.R. Ulrich (Wiley, New York, 1984) p. 113.
[16] B.E. Yoldas, J. Non-Cryst. Solids 63 (1984) 145.
[17] S. Sakka and K. Kamiya, J. Non-Cryst. Solids 48 (1982) 31.
[18] S. Sakka and H. Kozuka, J. Non-Cryst. Solids 100 (1988) 142.
[19] H. Kozuka, H. Kuroki and S. Sakka, J. Non-Cryst. Solids 100 (1988) 226.
[20] G. Orcel, J.L. Noguès and L.L. Hench, Mater. Res. Soc. Symp. Proc. 73 (1986) 35.
[21] M.L. Huggins, J. Am. Chem. Soc. 64 (1942) 1712.
[22] I. Artaki, M. Bradley, T.W. Zerda and J. Jonas, J. Phys. Chem. 89 (1985) 4399.
[23] B.E. Yoldas, J. Am. Ceram. Soc. 65 (1982) 387.
[24] B.E. Yoldas, J. Non-Cryst. Solids 51 (1982) 105.
[25] B.E. Yoldas, in: Ultrastructure Processing of Ceramics, Glasses, and Composites, ed. L.L. Hench and D.R. Ulrich (Wiley, New York, 1984) p. 60.
[26] H. Kozuka, S.H. Kim and S. Sakka, in: Ultrastructure Processing of Advanced Ceramics, ed. J.D. Mackenzie and D.R. Ulrich (Wiley, New York, 1988) p. 159.